Geochemistry Geophysics Geosystems G3
AN ELECTRONIC JOURNAL OF THE EARTH SCIENCES
Published by AGU and the Geochemical Society

Technical Brief
Volume 2
July 3, 2001
Paper number 2000GC000124
ISSN: 1525-2027

Determination of molybdenum isotope fractionation by double-spike multicollector inductively coupled plasma mass spectrometry

Christopher Siebert, Thomas F. Nägler, and Jan D. Kramers

Isotopengeologie, Mineralogisch-Petrographisches Institut, Universität Bern, CH-3012 Bern, Erlachstrasse 9a, Switzerland (siebert@mpi.unibe.ch; naegler@mpi.unibe.ch; kramers@mpi.unibe.ch)

[1] **Abstract:** Molybdenum isotopic compositions are precisely determined by MC-ICP-MS measurements using a Mo double spike. The double spike is added prior to chemical purification, so that laboratory and instrumental mass fractionations are separated from natural mass-dependent fractionation. Fractionation is determined on four Mo mass ratios, providing an internal consistency check. The external standard reproducibility is at 0.06 per mil on the $^{98}Mo/^{95}Mo$ ratio (2 standard deviation)). Using a normal microconcentric nebuliser with a cyclonic spray chamber, the minimum quantity of Mo is ~1 μg for high-precision results. A hydrothermal molybdenite shows fractionation of −0.3 per mil on the $^{98}Mo/^{95}Mo$ ratio relative to our standard (Johnson Matthey, 1000 μg/mL (±0.3%) ICP standard solution, lot 602332B). Fine-grained sediments show fractionation of 0.1 and −0.3 per mil on the $^{98}Mo/^{95}Mo$ ratio. The observed Mo isotope fractionation is small but resolvable with the presented high-resolution technique.

Keywords: Molybdenum; stable isotopes; double spike; MC-ICP-MS; biogeochemistry.

Index terms: Atmospheric composition and structure—evolution of the atmosphere; geochemistry—isotopic composition/chemistry; geochemistry—instruments and techniques; global change—biogeochemical processes.

Received November 30, 2000; **Revised** April 24, 2001; **Accepted** May 3, 2001; **Published** July 3, 2001.

Siebert, C., T. F. Nägler, and J. D. Kramers, 2001. Determination of molybdenum isotope fractionation by double-spike multicollector inductively coupled plasma mass spectrometry, *Geochem. Geophys. Geosyst.*, vol. 2, Paper number 2000GC000124 [4613 words, 8 figures, 4 tables]. Published July 3, 2001.

1. Introduction

[2] Molybdenum (Mo) is a redox-sensitive trace metal and becomes enriched in reducing, sulfidic, organic rich sediments. It is also essential for life, and therefore biological molybdenum isotopic fractionation is probable [e.g., *Sundius*, 1941; *Helz et al.*, 1996; *Morford and Emerson*, 1999, and references therein].

[3] Further, abiogenic Mo isotope fractionation may occur in terrestrial redox-sensitive processes. The style of chemical weathering may have an influence on both the Mo concentration and Mo isotopic composition of the eroded material. Because the solubility of Mo is dependent on the redox state, Mo concentrations and isotopic composition may provide a tool in quantifying redox condi-

tions in the early atmosphere as well as the extend of biological activity in a given paleo-environment. Another possible mechanism of isotope fractionation could occur when molybdenite is formed from a hydrothermal solution.

[4] Therefore Mo isotope fractionation analysis bears the potential of becoming an important geochemical tool for the study of a wide range of processes. The present study demonstrates why the double-spike technique is particularly suited to perform this type of study.

2. Analytical Methods and Considerations

[5] Generally, the determination of natural isotope fractionation of an element necessitates resolution of natural fractionation from fractionation that appears during (1) chemical purification and during (2) isotope measurements.

[6] Given the fact that Mo has seven stable isotopes (92, 94, 95, 96, 97, 98, 100) with relative abundances from 9 to 24%, application of a double spike is straightforward. The major advantages are the following: (1) Isotope fractionation during chemical separation can be accounted for [cf. *Russell et al.*, 1978]. Therefore priority can be given to high-purity Mo separation over a optimum yield separation. (2) Instrumental bias can be resolved from natural fractionation in the very same measurement on a single pure Mo run, provided that Mo isotopic anomalies other than mass-dependent fractionation are absent. This condition can further be tested by a measurement of an unspiked sample aliquot. Another significant advantage is that the double-spike technique provides molybdenum concentrations to a precision hardly obtainable by other methods.

[7] Thus this technique has advantages over other techniques used to determine natural isotope fractionation such as element doping and bracketing standards. The latter two provide no concentration information and rely on a fractionation-free chemical separation, i.e., approaching a 100% yield. Since the mass-dependent instrumental fractionation varies significantly with time, bracketing standards techniques require a sample/standard measuring time ratio approaching 1. In addition, the individual analysis time must be kept short, thus limiting the statistical basis. Element doping relies on the assumption that instrumental fractionation is identical for both the doped elements and the element to analyze [*Hirata*, 1996; *Belshaw et al.*, 1998; *Rehkämper and Halliday*, 1999; *Marechal et al.*, 1999; *White et al.*, 2000]. Further, isobaric interferences from matrix elements and molecules may occur on either the analyzed element and/or the element used for fractionation correction. Finally, the mass range to be analyzed must be extended to the doping element masses, which generally reduces the number of isotopes of the target element that can be analyzed. In the case of Mo, element doping with Zr (zirconium) or Ru (ruthenium) produces several isobaric interferences in eihter case. Element doping with Pd (paladium) would need an extention of the measured mass range by 30% to mass ^{104}Pd.

2.1. Double-Spike Design

[8] We have chosen masses ^{97}Mo and ^{100}Mo for the following reasons: (1) The relative abundance of ^{97}Mo and ^{100}Mo is low (9.55 and 9.63%) [*Parrington et al.*, 1996]. (2) There are no elemental isobaric interferences on mass 97. On mass 100, there is a potential ^{100}Ru interference, which, however, can easily be reduced (see below). (3) Highly enriched

^{97}Mo and ^{100}Mo can be obtained, for example, from Oak Ridge National Laboratory (94.2 and 97.2%).

2.2. Calibration of the Double Spike

[9] The double-spike composition was defined relative to a Mo standard (Johnson Matthey ICP standard solution, lot 602332B). Calibration results are given in Table 1.

[10] In a first calibration step (column 1 in Table 1) both pure standard and pure spike solutions were doped with Pd. The ^{100}Mo/^{97}Mo ratio was then defined applying an instrumental fractionation correction based on a ^{104}Pd/^{102}Pd ratio of 10.922 [*Parrington et al.*, 1996]. Masses 104 to 96 can be measured statically on the Nu instruments inductively coupled plasma mass spectrometer (MC-ICP-MS). Uncertainties of element doping procedures (see above) were kept to a minimum by the following measures:

[11] The ^{104}Pd/^{102}Pd ratio and the ^{100}Mo/^{97}Mo ratios of both solutions were measured with exactly the same routine and run parameters. Matrix effects as in geological samples are not to be expected, as both standard and spike represent pure Mo and were measured from the same pure medium. As the spike was designed to have a ^{100}Mo/^{97}Mo ratio very similar to the natural ratio, the intensities of ^{104}Pd, ^{102}Pd, ^{100}Mo, and ^{97}Mo could be kept at the same level in spike and standard measurements. The absolute ^{100}Mo/^{97}Mo ratio of the spike defined in this way is dependent on the Pd ratio used. However, the ^{100}Mo/^{97}Mo ratio of the spike is precisely defined relative to the standard ^{100}Mo/^{97}Mo ratio.

[12] In a second calibration step all other Mo isotopic ratios of the spike (and standard) were defined in pure Mo runs by correcting for instrumental mass bias via the respective ^{100}Mo/^{97}Mo ratio as described below (columns 2–6 in Table 1). Finally, spike standard mixtures of varying relative proportions were measured in pure Mo runs to test accuracy of the calibration (see section 4).

3. Mass Spectrometry

[13] Measurements were carried out with a double-focusing Nu Instruments MC-ICP-MS system (Wrexham, North Wales, United Kingdom). An electrostatical analyser (ESA) placed before the magnet focuses the ion beam with a high-energy dispersion inherited from the plasma source. Two electrostatic lenses placed after the magnet enable the dispersion of the ion beams to be varied, making multicollector measurements in a fixed array of 12 Faraday collectors and three electron multipliers possible.

[14] Standards and samples are taken up in 0.35N HNO_3. Analytes are nebulized using a

Table 1. Results of Spike and Standard Calibration Measurements[a]

$^{100/97}$Mo[b]	2 s.d.	$^{98/97}$Mo[c]	2 s.d.	$^{96/97}$Mo[c]	2 s.d.	$^{95/97}$Mo[c]	2 s.d.	$^{94/97}$Mo[c]	2 s.d.	$^{92/97}$Mo[c]	2 s.d.
Spike											
0.903695	8E-05	0.044564	2E-05	0.016374	5E-06	0.007773	2E-05	0.003719	2E-06	0.007399	5E-06
Standard											
1.00313	1E-05	2.52293	7E-04	1.74771	6E-04	1.67182	6E-04	0.97246	4E-04	1.56519	6E-04

[a]Read 8E-05 as 8×10^{-5}.

[b]Normalized to $^{104/102}$Pd = 10.922.

[c]Normalized to $^{100/97}$Mo of spike = 0.903695 ± 8exp-5 (2 s.d.); normalized to $^{100/97}$Mo of standard = 1.003133 ± 2exp-5.

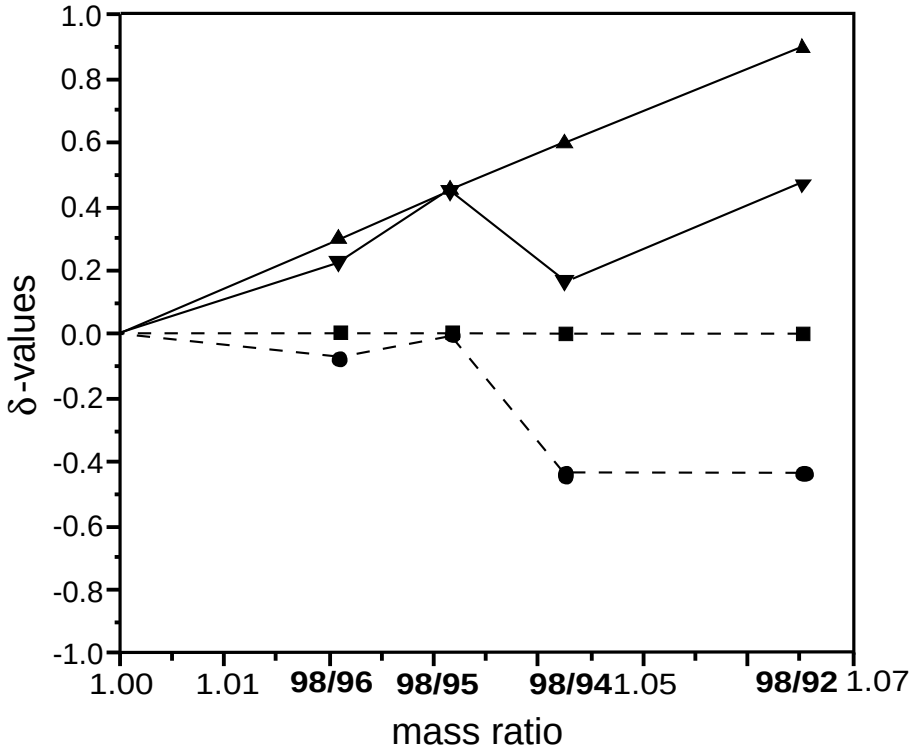

Figure 1. Calculated effect of a Zr interference on theoretical data. Two examples are indicated by solid and dashed lines, respectively. Straight lines are compositions without interference, lines with deviations are same compositions with Zr interference.

Micromist low-uptake nebulizer (50 μL/min) with a water-cooled cyclonic spray chamber (Glass Expansion, Camberwell, Victoria, Australia) at −2°C. Typical analyte Mo contents are 1–3 μg. After each run, the nebulizer and spray chamber are rinsed with 0.35N HNO_3 followed by H_2O and again 0.35N HNO_3 until normal background is reached (generally after 4 min). First experiments with an Aridus® (Cetac) desolvating nebulizer indicate that the necessary sample size can be reduced by a factor of 10.

[15] Measurements are performed using 8 of 12 Faraday collectors in static mode. Masses 92, 94, 95, 96, 97, 98, 99 (Ru monitor), and 100 are measured simultaneously. Integration time for each cycle is set at 10 s. Magnet settle time is set to 6 s. A measurement usually consists of 5 blocks with 10 cycles each. Total ion currents during sample analysis are around 5exp-11A. Background is measured for 15 s before every block by deflection of the ESA. In addition, the magnet is set off half a mass unit. Background reproducibility is at 1 mV for 1/10 s integration and at 0.01 mV for 10 s integration, respectively.

3.1. Isobaric Interferences

3.1.1. Ru

[16] Isobaric interferences on Mo masses are possible from Ru isotopes 96 (5.52% relative abundance), 98 (1.88%), and 100 (12.6%). However, the Ru/Mo ratio in terrestrial samples

is very low, and Ru can be chemically separated from Mo. In addition, the presence of Ru can easily be monitored and corrected for within run using mass 99 (12.7%). For samples with potential Ru isotopic anomalies (e.g., meteorites) the chemical Mo purification procedure must completely remove Ru.

3.1.2. Zr

[17] Isobaric Mo and Zr isotopes are 92 (17.15% relative abundance of Zr), 94 (17.38%), and 96 (2.8%). Tests for the presence of Zr interferences can be made on mass 90 (51.45% of total Zr) pre- and/or postrun. In addition, the different relative amounts of Zr isotopes would lead to internally inconsistent results for the determined Mo ratios. In Figure 1 the effects of a Zr interference are shown for two hypothetical samples. Ratios of Zr-free Mo isotopes (^{100}Mo, ^{98}Mo, ^{97}Mo, and ^{95}Mo) are still correct. In order to realize the full potential of the method it is a prerequisite to remove Zr efficiently from geological material. In addition, analytes must be handled in HF-washed equipment.

3.2. Data Reduction

[18] In this work we have assumed that both instrumental and natural mass-dependent fractionation follow an exponential law. For the instrumental fractionation this is robustly supported by isotope work on Nd and Os where internal fractionation correction is applied [*Schoenberg et al.*, 2000; *von Blankenburg and Nägler*, 2001]. For the natural fractionation it conforms to the assumption normally made in light stable isotope studies.

[19] A three-dimensional data reduction procedure similar to that described by *Hofmann* [1971] and *Johnson and Beard* [1999] is carried out online. Thereby we make use of three isotope ratios with the same mass as common denominator (Figure 2). In the three-dimensional data reduction, straight lines and flat planes are used to determine intercepts which yield fractionation factors. This approach allows simple mathematics but does not correspond to the exponential fractionation law, in which fractionation is described by a curve [see, e.g., *Johnson and Beard*, 1999]. This problem has been solved by finding lines and flat planes by iteration, for which intercepts correspond to the true intercepts of the fractionation curve. See Appendix A for a detailed description.

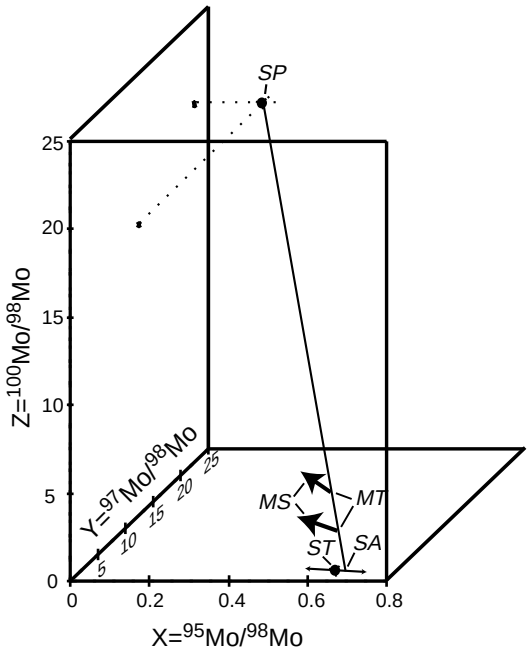

Figure 2. Sketch of sample and spike isotope ratios in the space $X = {}^{95}\mathrm{Mo}/{}^{97}\mathrm{Mo}$, $Y = {}^{97}\mathrm{Mo}/{}^{98}\mathrm{Mo}$, $Z = {}^{100}\mathrm{Mo}/{}^{98}\mathrm{Mo}$. Scale of x is magnified compared to the others. SP, spike; ST, standard; SA, sample ("fractionated standard"); MT, true composition of spike-sample mixture (two examples shown); MS, measured (spike-sample mixture after instrumental fractionation); SP-SA, mixing line; thin double-headed arrow, approximate direction of natural fractionation relative to the standard, i.e., the locus of Mo isotopic fractionation in natural samples; thick single-headed arrows, approximate direction of instrumental fractionation; dotted lines indicate the spike composition.

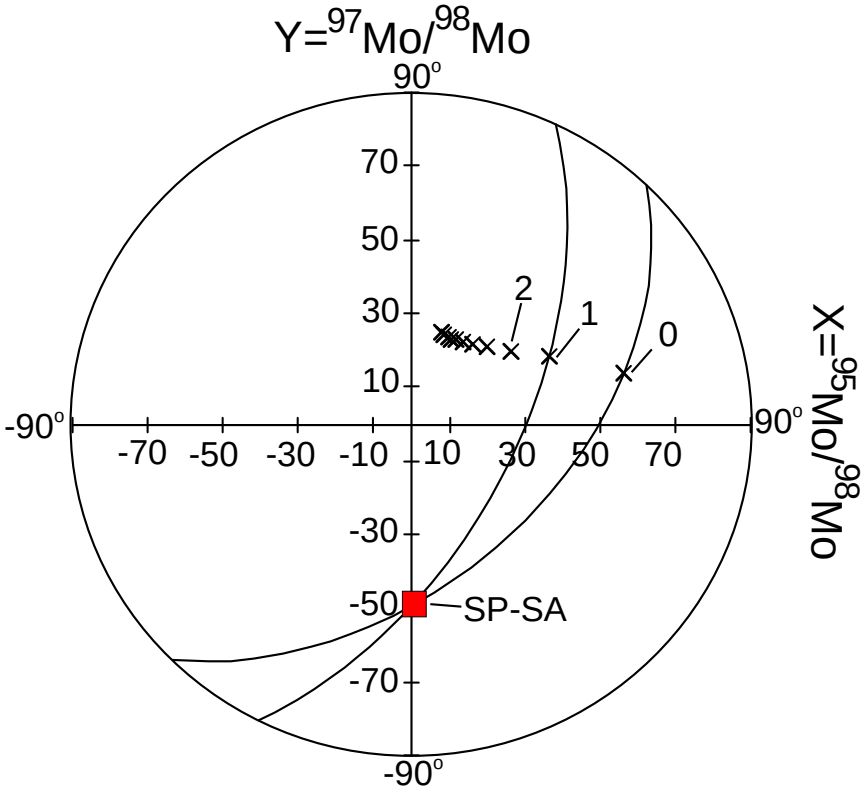

Figure 3. Lower hemisphere true-angle stereographic plot (z axis is perpendicular to drawing plane) showing the direction of sample-spike mixing line (SP-SA) and fractionation "lines" (shown as crosses), i.e., lines through "true" (unfractionated) and fractionated (instrumental fractionation factor is 2) mixtures. Point 0, pure standard (approximately natural fractionation); 1 and 2, $^{100}Mo_{spike}/^{100}Mo_{sample}$ = 1 and 2, respectively, with further crosses at increments of 1. Great circles are traces of planes parallel to *SP-SA-ST* (arc through point 0) and *SP-MT-MS* (arc through point 1; see Figure 2). It can be seen that no low angle intersections are generated in the data reduction if $^{100}Mo_{spike}/^{100}Mo_{sample} \approx 1$ or greater, which explains the precision achieved by isotope dilution.

[20] An important issue for the precision of the isotope ratio determination is the intersection angles of the involved trajectories, as very oblique intersections would produce significant error amplifications. In Figure 2 the isotope ratios and mixing line between spike and sample are plotted. The way in which the direction of fractionation changes with varying spike to sample ratios is shown semiquantitatively. From Figure 3 it can be seen that the angle between the direction of fractionation of a given sample and the sample-spike mixing line is always in excess of 70°. Further, the direction of fractionation changes rapidly as spike is added to sample: for a ratio of $^{100}Mo_{spike}/^{100}Mo_{sample}$ = 1 (point 1 in Figure 3) the direction already differs more than 20° from the fractionation direction of the pure sample (point 0), and it can be seen that the angle between planes *SP-MS-MT* and *SP-SA-ST* is similarly large. These angles increase (and thus error magnification caused by low angle intersections is reduced) as more spike is added, and is predicted to compensate a larger error magnification resulting from projection from the point *SP* (Figure 2), so that overall

precision should not change much for a large range of spike to sample ratios. This has indeed been confirmed (see section 4).

3.3. Delta Notation

[21] As mentioned before, absolute abundances or isotope ratios defined with this method are dependent on the assumed Pd isotopic composition used in the first step of the spike and standard isotope calibration. Therefore relative variations of Mo isotopic compositions can be defined significantly more accurate, and consequently, we present our data in $^{98/x}\delta$ notations defined as

$$\delta^{98}/^{x}\mathrm{Mo} = \{[(^{98}\mathrm{Mo}/^{x}\mathrm{Mo})_{\mathrm{sample}} - (^{98}\mathrm{Mo}/^{x}\mathrm{Mo})_{\mathrm{standard}}] / [(^{98}\mathrm{Mo}/^{x}\mathrm{Mo})_{\mathrm{standard}}] \times 1000\},$$

where ^{x}Mo represents isotopes ^{96}Mo, ^{95}Mo, ^{94}Mo, and ^{92}Mo, respectively. The subscript standard refers to the data of our in-house standard (see above), which are used for online δ calculations. For interlaboratory comparison, aliquots of the standard are available from the authors. Mass 98 was chosen as reference, as it is the most abundant natural Mo isotope and no isobaric Zr exists. Molybdenum 98 is used as numerator to be consistent with other stable isotope systems. For presentation of standard reproducibility and general data comparisons we use the ^{98}Mo/^{95}Mo ratio, because both masses are free from isobaric interferences and have the same mass difference as the spike isotopes.

[22] As far as mass-dependent natural isotopic fractionation is concerned, the delta values of the different Mo isotopic ratios must correlate with their mass ratio: $^{98}\mathrm{Mo}/^{x}\mathrm{Mo} \sim 98/x$. Therefore, in a two-dimensional diagram of mass ratios versus δ values, an exponential curve must result within analytical error. Because the bending of this curve would be negligible with respect to the instrumental resolution, the trajectory can be simplified to a straight line. Unresolved molecular isobaric interferences would result in a nonlinear distribution (see also above). An obvious consistency test results from the fact that the line necessarily must pass through $^{98/98}\delta = 0$.

Table 2. Mo Standard Measurements[a]

Date	$\delta^{98/96}$Mo	$\delta^{98/95}$Mo	$\delta^{98/94}$Mo	$\delta^{98/92}$Mo
March 22, 2000	0.01	0.00	−0.04	−0.02
March 22, 2000	−0.01	−0.02	−0.05	−0.16
March 22, 2000	−0.05	−0.04	−0.10	−0.13
March 22, 2000	−0.02	−0.06	−0.09	−0.13
March 22, 2000	−0.03	−0.03	−0.05	−0.14
March 22, 2000	0.05	0.09	0.14	0.27
March 22, 2000	−0.01	0.00	0.05	−0.04
March 22, 2000	−0.02	−0.04	−0.05	−0.16
March 22, 2000	0.01	0.00	0.07	0.07
March 22, 2000	0.04	0.06	−0.04	0.01
March 22, 2000	−0.02	−0.02	−0.03	0.12
2 s.d. of day	0.06	0.09	0.14	0.26
March 23, 2000	0.06	−0.06	0.14	0.23
March 23, 2000	0.01	0.01	0.01	0.02
March 23, 2000	−0.02	0.00	−0.03	−0.04
March 23, 2000	−0.01	−0.01	−0.02	−0.04
March 23, 2000	0.01	0.05	0.09	0.15
2 s.d. of day	0.05	0.07	0.14	0.22
March 29, 2000	−0.05	−0.05	−0.01	−0.06
March 29, 2000	0.01	0.04	−0.05	0.00
March 29, 2000	0.04	0.02	0.05	0.06
2 s.d. of day	0.08	0.08	0.08	0.09
May 3, 2000	−0.01	−0.05	−0.03	−0.01
May 3, 2000	0.01	0.03	0.03	−0.03
May 3, 2000	0.00	0.02	0.00	0.04
2 s.d. of day	0.01	0.07	0.05	0.06
June 22, 2000	0.01	0.04	0.14	0.22
June 22, 2000	0.03	0.06	0.13	0.18
June 22, 2000	0.01	−0.07	−0.14	−0.11
June 22, 2000	0.01	0.04	−0.02	−0.04
June 22, 2000	−0.07	−0.11	−0.11	−0.17
June 22, 2000	0.00	0.04	0.00	−0.09
2 s.d. of day	0.06	0.12	0.21	0.30
August 29, 2000	0.03	0.05	0.03	0.07
August 29, 2000	−0.01	−0.04	−0.03	−0.02
August 29, 2000	−0.03	−0.01	−0.01	−0.05
2 s.d. of day	0.05	0.08	0.05	0.10
Average all data	0.00	0.00	0.00	0.00
2 s.d. all data	0.03	0.04	0.07	0.12

[a]Standard measurements over a period of 6 month, showing the variations within each session. The given data are corrected with the average standard value of the respective day (see Figure 3 and section 4).

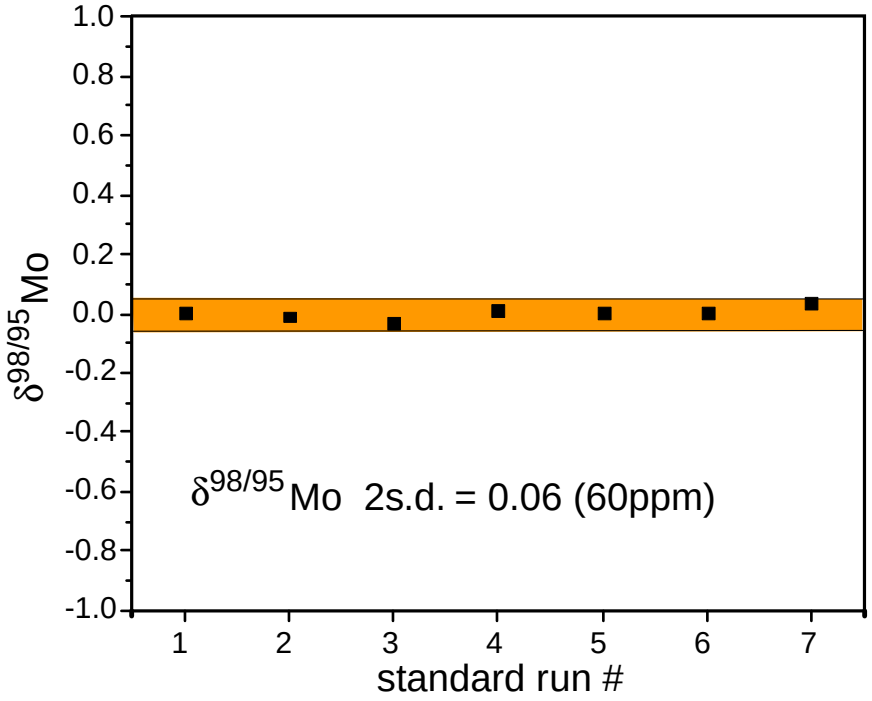

Figure 4. Plot of $\delta^{98/95}$Mo versus standard measurements within one session. Within-run precision is less than or equal to the symbol size (error frame indicates external reproducibility (2 standard deviation)).

3.4. Chromatography

[23] Digested samples are diluted in 2N H_2SO_4 with 0.1% H_2O_2 added. For the ion exchange procedure columns containing 1 cm^3 Dowex AG1 (200–400 mesh) anion exchange resin are used. The resin is conditioned with two column volumes of H_2SO_4. The sample solutions are then put on the columns. After rinsing with four column volumes (V) with the H_2SO_4-H_2O_2 mixture, the remaining foreign elements are eluted with $2V$ 2M HNO_3. The Mo fraction is eluted by $4V$ 2M HNO_3. In the case of very Fe- and/or Ru-rich samples the procedure is repeated using $10V$ of H_2SO_4/H_2O_2 mixture and $10V$ of 1M HCl. The Mo fraction is then eluted by $7V$ $1M$ HCl. The samples are diluted in 0.35M HNO_3 for ICP measurements. The procedure shows a >90% yield on standard solutions. Total blanks are below 5 ng. They are mainly due to single distilled (HNO_3, HCl) or off shelf (H_2SO_4, H_2O_2) reagents used.

4. Results and Discussion

[24] The results of standard measurements from several measuring sessions are shown in Table 2. Within individual measurement sessions (1–2 days) spiked standard solutions show 2 standard deviation reproducibilities between 0.02 and 0.12 per mil (20 and 120 ppm, respectively) on ratio $^{98}Mo/^{95}Mo$ (Table 2 and Figure 4).

[25] Figure 5 shows deviations of mean standard values over time from the calibration value. It is obvious that the deviations of the measured standard values and errors vary between different measuring sessions. The scatter is not mass dependent. For all

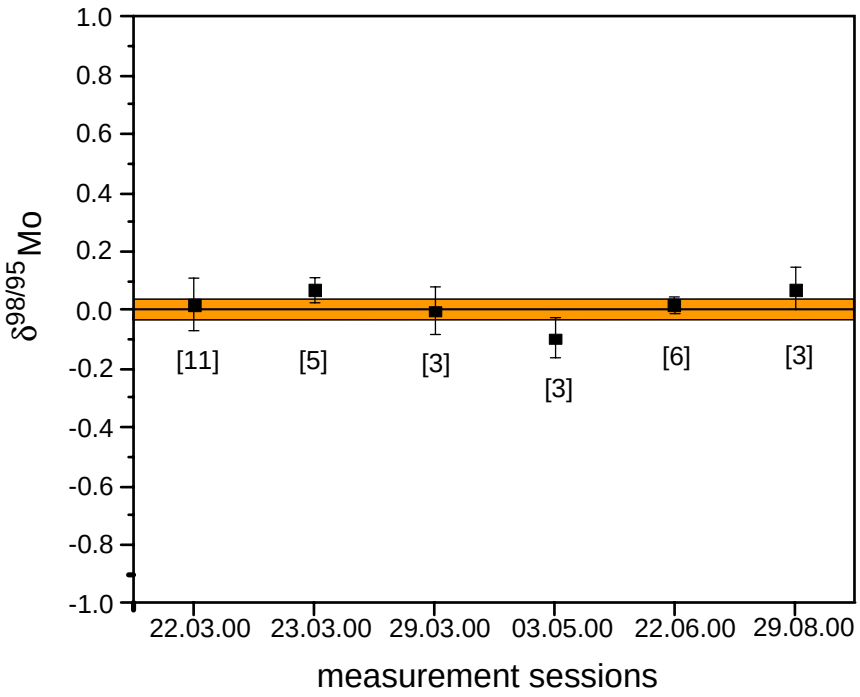

Figure 5. Plot of mean $\delta^{98/95}$Mo standard values as measured of six measurement sessions. Numbers in brackets are numbers of standards analyzed. Because the deviations of standard values and errors vary between different measuring sessions, every individual standard and sample measurement is subsequently normalized to the mean standard value of the session. The resulting mean long-term external standard reproducibility (Table 2) is 0.04 per mil (2 standard deviation) for the ^{98}Mo/^{95}Mo ratio (error frame).

ratios but ^{98}Mo/^{94}Mo, long-term variations are similar as session uncertainties. In some sessions, unsystematic deviations in particular of the ^{98}Mo/^{94}Mo ratio from the calibrated standard values exceeded analytical uncertainties. This is due to minute Zr interferences, occurring as memory from MC-ICP-MS measurements of other elements. Zr contributions were too low to be significant except for mass 94, the mass with the highest Zr/Mo ratio. To account for the observed variations between sessions, standard and sample measurements are normalized to the mean standard value of the session. Mean long-term external standard reproducibility of these corrected values (Table 2) is 0.04 per mil (2 standard deviation) for the ^{98}Mo/^{95}Mo ratio.

[26] From the results of standard measurements with different spike/standard ratios (expressed by the ^{97}Mo/^{98}Mo ratio) shown in Figure 6, it is clear that varying spike/sample ratios up to a ^{97}Mo/^{98}Mo ratio of ~10 (spike ^{97}Mo/^{98}Mo ratio is ~22.5) have no influence on the accuracy of the measurements showing the accuracy of double-spike calibration and data reduction. In addition, only the order of magnitude of Mo contents of samples must be known prior to spiking. Since Mo concentrations may vary significantly between similar geological materials, the possibility of analyzing a wide range of spike/sample ratios is desirable.

[27] In Figure 7 the molybdenum isotopic composition of our standard solution is compared to

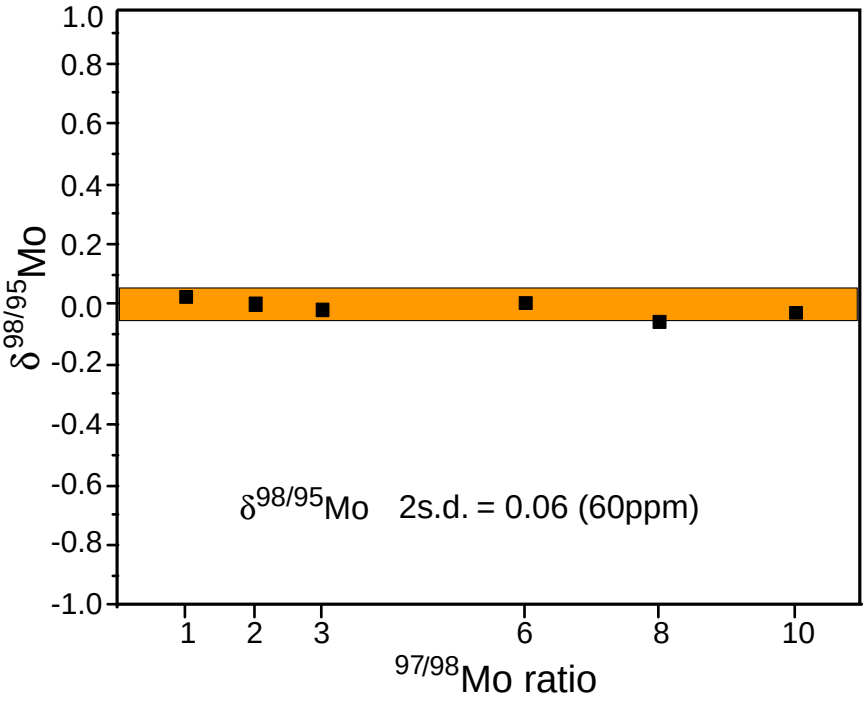

Figure 6. Plot of $\delta^{98/95}$Mo versus spike/standard ratio, expressed by the ^{97}Mo/^{98}Mo ratio, which clearly demonstrates that any inaccuracy in spike composition is insignificant for accuracy of measurements (at least for spike/sample ratios up to 10). Error frame as in Figure 4.

the data of *Lee and Halliday* [1995] (MC-ICP-MS) and *Wieser and De Laeter* [2000] (TIMS). The linear arrangement of the data sets shows that the differences are dominantly mass dependent, resulting from the different normalisation procedures used.

[28] As argued above, Mo isotopic fractionation may occur during Mo separation. Unspiked Mo standard aliquots eluted successively from an anion exchange column and spiked only subsequently showed deviations of up to 1.6 per mil on 5% fractions for the ^{98}Mo/^{95}Mo ratio (Table 3). *Marechal et al.* [1999] also observed a substantial fractionation of copper (Cu) isotopes (up to 9.7 per mil between the first and last cut) on anion exchange column. *Anbar et al.* [2000] reported this effect for iron (Fe) arguing that this fractionation reflects equilibrium fractionation between different Fe-chloride complexes. Similar effects may, in principle, be present in Mo anion exchange separation. *Kraus et al.* [1955] deduced from their observations of two clearly separated Mo elution maxima that at least two species of Mo(VI) exist in weak hydrochloric acid (<1M HCl). They attributed this to the rather complicated hydrolytic behavior of Mo(VI). In addition, *Strelow and Bothma* [1967] noted the tendency of Mo(VI) to form polynuclear species in higher H_2SO_4 concentrations. However, as demonstrated by the same authors in the presence of H_2O_2, polymolybdate ion formation is suppressed by peroxide complex formation. We thus stabilized our Mo(VI) by the addition of H_2O_2. Further, all acids used during our Mo separation are minimum 1M. Owing to these pre-

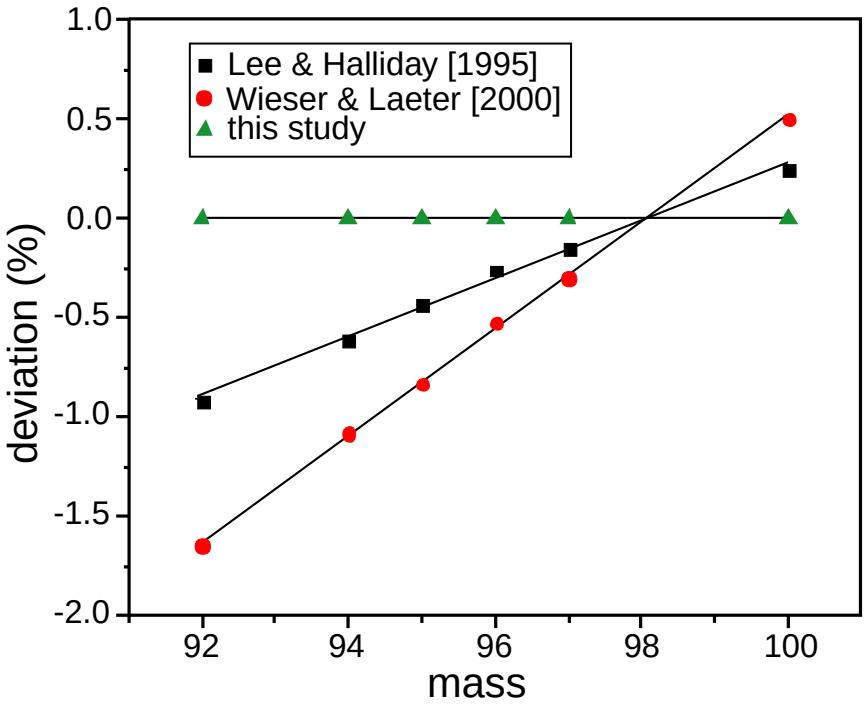

Figure 7. Comparison of molybdenum isotopic composition of our standard solution with the data of *Lee and Halliday* [1995] (MC-ICP-MS) and *Wieser and De Laeter* [2000] (TIMS). Errors (2 standard deviation) are within symbol size. Differences between all three data sets are dominantly mass-dependent variations, caused by different normalization procedures.

cautions, the potential for the existence of two different Mo(VI) species is demagnified, and also a single Mo elution maxima is observed. In addition, even in the absence of complexations, ions of a single speciation can be fractionated on ion exchange columns [e.g., *Russell et al.*, 1978]. The order of Mo isotope elution may simply reflect subtle differences in the partition coefficients of the light and heavy Mo isotopes and the resin. In all

Table 3. Mo Isotope Fractionation on the Column

HNO_3[a], mL	Fraction,[a] %	$\delta^{98/95}Mo$[a]	HNO_3[b], mL	$\delta^{98/95}Mo$[b]
2.4–2.8	4.3	−1.61	2.5–3.0	0.01
2.8–3.0	2.2	−1.34	3.0–3.5	0.02
3.0–3.5	8.4	−0.56	3.5–4.0	0.03
3.5–4.5	52.5	−0.12	4.0–4.4	0.02
4.5–4.8	6.5	0.23	4.4–4.8	0.07
4.8–5.2	7.6	0.35	4.8–5.2	0.04

[a]Data from unspiked Mo standard aliquots eluted successively from an anion exchange column and spiked only subsequently. During this experiment the tailing of Mo was not totally captured. The mass balance indicates that the omitted 18.5% of Mo must have had a $\delta^{98/95}Mo$ of 0.9.

[b]Prespiked alliquots demonstrate that fractionation on the column is accounted for by the double spike technique.

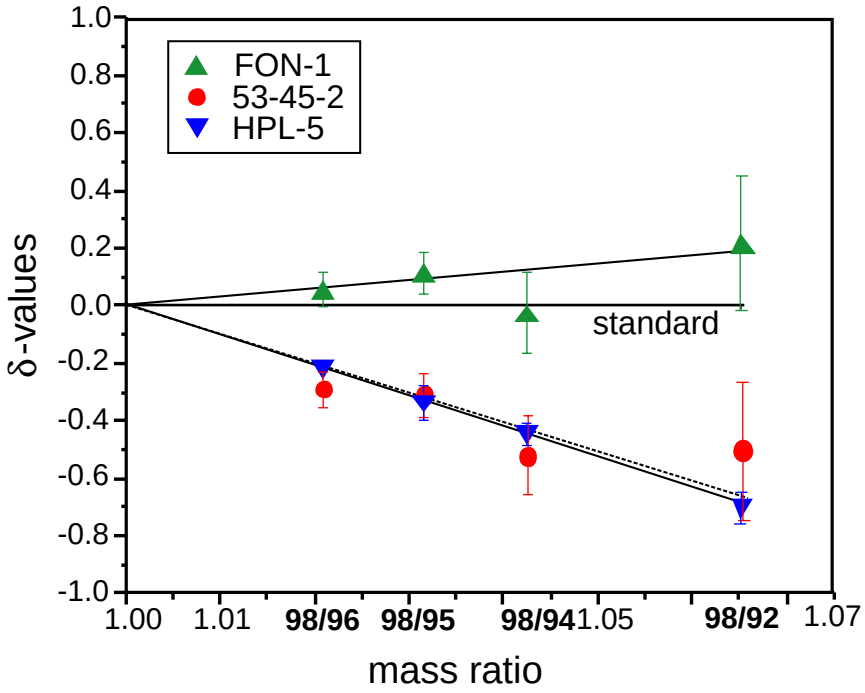

Figure 8. Plot of measured delta values versus Mo isotope mass ratios showing natural mass-dependent fractionation (mass-dependent fractionation of sample 53-45-2 is indicated by a dotted line to differentiate it from sample HPL-5). The relatively higher errors of some sediment delta values are due to minute Zr contributions (see text for explanation). However, almost all delta values plot within errors on a line through the (Zr free) $^{98}Mo/^{95}Mo$ and $^{98}Mo/^{98}Mo$ ratios.

circumstances the problem is analytically solved by adding the double spike before chemical separation (Table 3). Subsequent artificial fractionation affects both sample Mo and spike Mo in a mass-dependent manner. Within the resolution of measurements, fractionation on the column and in the mass spectrometer follow the same exponential law and can be reduced mathematically.

[29] Hydrothermal molybdenite from Huanglongpu, China (HLP-5 [*Stein et al.*, 1997]) shows significantly lighter isotopic composition of $\delta^{98/95}Mo$ −0.3 with respect to our standard (Figure 8 and Table 4). This difference may, however, be introduced during technical purification processes of the Mo used for the standard. However, analyzed fine-grained sediments (FON-1 [*Nägler et al.*, 1995]; sam-

Table 4. Results of Sample Measurements

Sample	$\delta^{98/96}Mo$	2 s.d.	$\delta^{98/95}Mo$	2 s.d.	$\delta^{98/94}Mo$	2 s.d.	$\delta^{98/92}Mo$	2 s.d.
53-45-2	−0.29	0.06	−0.30	0.07	−0.52	0.14	−0.50	0.24
FON-1	0.04	0.06	0.10	0.07	−0.04	0.14	0.20	0.24
HLP-5	−0.22	0.01	−0.33	0.07	−0.44	0.05	−0.69	0.06

ple 53-45-2, U.S. Geological Survey Cruise RP-8-OC-75; Table 4) show significant differences relative to the natural molybdenite (FON-1: $\delta^{98/95}$Mo 0.43) and to each other ($\delta^{98/95}$Mo of 0.4), thus demonstrating terrestrial fractionation of Mo isotopes. The $\delta^{98/95}$Mo of both samples were reproduced within 0.1 per mil. Therefore the observed Mo isotope fractionations are clearly resolvable. The relatively higher deviations of some delta values (and the higher 2 standard deviation errors) are due to minute Zr contributions (see above). However, almost all delta values plot within errors on a line through the (Zr unaffected) ^{98}Mo/^{95}Mo and ^{98}Mo/^{98}Mo ratios showing consistency (Figure 8).

5. Conclusions

[30] MC-ICP-MS measurements with double-spike technique provide high-resolution Mo isotopic fractionation determinations. On a Nu instrument ICP, molybdenum masses 92 through 100 can be measured statically.

[31] Applying a ^{100}Mo/^{97}Mo double-spike, isotopic fractionation can be defined on mass ratios 98/96, 98/95, 98/94, and 98/92.

[32] If these ratios are plotted versus their corresponding deviation from standard (δ values), a straight line passing through 0 for mass ratio 1 must result within analytical error. Thus consistency of the results can be checked, and possible isobaric interferences can be detected.

[33] A single, double-spiked measurement provides precise and accurate results on isotopic composition and Mo concentrations of an unknown sample.

[34] In view of the clearly resolvable natural variations observed, Mo isotope determination by double-spike technique and MC-ICP-MS has great potential to provide constraints on a wide variety of geological and cosmochemical problems.

Appendix A. Detailed Description of the Instrumental Fractionation Correction Procedure

[35] The fractionation law used states

$$R_{\text{measured}} = R_{\text{true}}\left(\frac{m_1}{m_2}\right)^F \text{(instrumental fractionation)} \tag{A1}$$

or

$$R_{\text{sample}} = R_{\text{standard}}\left(\frac{m_1}{m_2}\right)^F \text{(natural fractionation)}, \tag{A2}$$

where F is the exponential fractionation factor, R is the abundance ratio of isotopes with masses m_1 and m_2. If $m_1 > m_2$, then $F > 0$ describes a fractionation favoring the heavier isotope, such as in ICP-MS. For the Nu Instruments machine, $F \approx 2$ normally.

[36] For data reduction an x-y-z coordinate system is used in which axes are assigned to isotope abundance ratios as follows:

$$x = \mathrm{N}^{95}\mathrm{Mo}/\mathrm{N}^{98}\mathrm{Mo}$$
$$y = \mathrm{N}^{97}\mathrm{Mo}/\mathrm{N}^{98}\mathrm{Mo}$$
$$z = \mathrm{N}^{100}\mathrm{Mo}/\mathrm{N}^{98}\mathrm{Mo}.$$

Isotope ratios are denoted Rx, Ry, and Rz, with subscripts SA (sample), ST (standard), SP (spike), MS (measured), and MT (measured, corrected for instrumental fractionation). Fractionation factors are denoted F_{nat} (natural fractionation relative to the standard) and F_{ins} (instrumental fractionation).

A.1. Step 1

[37] A value for F_{nat} relative to the standard is assumed (arbitrary but best between -1 and 1 as true fractionation is most likely in that range). Together with the isotope ratios of the

standard, this value is used to define a first assumed isotope composition of the sample ("fractionated standard"), for example, for the $N^{95}Mo/N^{98}Mo$ ratio

$$Rx_{SA} = Rx_{ST}\left(\frac{94.905}{97.905}\right)^{F_{nat}} \quad \text{(A3)}$$

and analogous for the other ratios. Together with the isotope ratios of the spike, those of standard and sample define a plane in which the true isotope composition of the spike-standard mixture should lie if the assumed value for F_{nat} were correct. This plane has the equation $z = ax + by + c$ and parameters a, b, and c are obtained by

$$a = \frac{Ry_{sta}(Rz_{sa} - Rz_{sp}) + Ry_{sa}(Rz_{sp} - Rz_{st}) + Ry_{sp}(Rz_{st} - Rz_{sa})}{Ry_{sta}(Rx_{sa} - Rx_{sp}) + Ry_{sa}(Rx_{sp} - Rx_{st}) + Ry_{sp}(Rx_{st} - Rx_{sa})}$$

$$b = \frac{Rx_{sta}(Rz_{sa} - Rz_{sp}) + Rx_{sa}(Rz_{sp} - Rz_{st}) + Rx_{sp}(Rz_{st} - Rz_{sa})}{Rx_{sta}(Ry_{sa} - Ry_{sp}) + Rx_{sa}(Ry_{sp} - Ry_{st}) + Rx_{sp}(Ry_{st} - Ry_{sa})}$$

$$c = Rz_{st} - aRx_{st} - bRy_{st}. \quad \text{(A4)}$$

A.2. Step 2

[38] A value for F_{ins} is assumed (in our case = 2, as this is the commonly observed value), and assumed "unfractionated isotope ratios" Rx_{MT}, Ry_{MT}, and Rz_{MT} for the measured sample-spike mixture are calculated analogous to (A1) (but using the negative value of F_{ins} since "true" ratios are calculated from the measured, fractionated ones). The isotope ratios of the "true" and measured mixture define a line. If values for F_{nat} and F_{ins} are both correct, this line should intercept the plane defined by ST, SA, and SP at the same point in space as the true exponential fractionation curve through the measured isotope ratios. The line is defined by two equations: $z = dx + e$ and $z = fy + g$. Parameters d, e, f, and g are found by

$$d = \frac{Rz_{MS} - Rz_{MT}}{Rx_{MS} - Rx_{MT}}$$

$$e = Rz_{MS} - dRx_{MS}$$

$$f = \frac{Rz_{MS} - Rz_{MT}}{Ry_{MS} - Ry_{MT}}$$

$$g = Rz_{MS} - fRy_{MS}. \quad \text{(A5)}$$

The coordinates x_{int}, y_{int}, and z_{int} of the intersection of a line ($z = dx + e$ and $z = fy + g$) with a plane ($z = ax + by + c$) are given by

$$x_{int} = \frac{bg - be + ef - cf}{af + bd - df}$$

$$y_{int} = \frac{ae - ag + dg - cd}{af + bd - df}$$

$$z_{int} = ax_{int} + by_{int} + c. \quad \text{(A6)}$$

Now the values Rx_{MT}, Ry_{MT}, and Rz_{MT} are set equal to these intercept values found, and a new value for F_{ins} is calculated following the exponential fractionation law (see (A3)).

$$F_{ins} = \frac{\ln(Rx_{MS}/Rx_{MT})}{\ln(94.905/97.905)} \quad \text{(A7)}$$

With this new value for F_{ins}, calculations under step 3 are reiterated. Results converge after two iterations.

A.3. Step 3

[39] The point MT, if true, is on a mixing line between SP and the true sample composition SA. However, point MT can only be correct if the plane ST-SA-SP (step 1) is correctly defined. In step 1 this was done using an assumed value of F_{nat}. A better value is now found as follows: A plane is defined through points MS, MT, and SP (analogous to (A4)). A "fractionation line" through the standard isotope composition ST is defined using the originally assumed F_{nat} value (analogous to (A5)). This "fractionation line" is intersected with the plane MS, MT, and SP (analogous to (A6)). The resulting x_{int}, y_{int}, and z_{int} are the new values for Rx_{SA}, Ry_{SA}, and Rz_{SA}. Using this new point for

SA, a new value for F_{nat} is calculated analogous to (A7). Following step 3, the complete procedure is repeated from step 1, including the iterations of step 2. The value for F_{nat} converges after two of these complete iterations. All other Mo ratios are fractionation corrected with the above calculated instrumental fractionation factor (F_{ins}).

[40] In principle, methods of two nested iterations are risky. However, in this case the system always converges (instead of swinging out of control) because F_{nat} is relatively small and errors in the slope of the "fractionation line" due to incorrect initial assumptions for this parameter are also minor. In practice the procedure is carried out on-line for each individual static multicollector measurement, so that no further error propagation calculations have to be applied to the standard deviation or standard error of the end results.

Acknowledgments

[41] This project was funded by the Swiss National Foundation (grant 20-61933.00). H. Stein and J. Hein are thanked for the samples HPL-5 and 53-45-2, respectively. The critical comments of two anonymous reviewers helped significantly to improve the quality of the manuscript.

References

Anbar, A. D., J. E. Roe, J. Barling, and K. H. Nealson, Nonbiological fractionation of iron isotopes, *Science*, *288*(5463), 126–128, 2000.

Belshaw, N. S., P. A. Freedman, R. K. O'Nions, M. Frank, and Y. Guo, A new variable dipersion double-focussing plasma mass spectrometer with performance illustrated for Pb isotopes, *Int. J. Mass Spectrometry Ion Proc.*, *181*, 51–58, 1998.

Helz, G. R., C. V. Miller, J. M. Charnock, J. F. W. Mosselmans, R. A. D. Pattrick, C. D. Garner, and D. J. Vaughan, Mechanism of molybdenum removal from the sea and its concentration in black shales: EXAFS evidence, *Geochim. Cosmochim. Acta*, *60*(19), 3631–3642, 1996.

Hirata, T., Lead isotopic analysis od NIST standard reference materials using multiple collector-inductively coupled plasma mass spectrometry coupled with modified external correction method for mass disscrimination effect, *Analyst*, *121*, 1407–1411, 1996.

Hofmann, A., Fractionation corrections for mixed-isotope spikes of Sr, K, and Pb, *Earth Planet. Sci. Lett.*, *10*, 397–402, 1971.

Johnson, C. M., and B. L. Beard, Correction of instrumentally produced mass fractionation during isotopic analysis of Fe by thermal ionisation mass spectrometry, *Int. J. Mass Spectrometry*, *193*, 87–99, 1999.

Kraus, K. A., F. Nelson, and G. E. Moore, Anion-exchange studies, XVII, Molybdenum(VI), tungsten(VI) and uranium(VI) in HCl and HCl-HF solutions, *J. Am. Chem. Soc.*, *77*, 3972–3977, 1955.

Lee, D.-C., and A. N. Halliday, Precise determinations of the isotopic compositions and atomic weights of molybdenum, tellurium, tin and tungsten using ICP magnetic sector multiple collector mass spectrometry, *Int. J. Mass Spectrometry Ion Proc.*, *146/147*, 35–46, 1995.

Marechal, C. N., P. Telouk, and F. Albarede, Precise analysis of copper and zinc isotopic compositions by plasma-source mass spectrometry, *Chem. Geol.*, *156*, 251–273, 1999.

Morford, J. L., and S. Emerson, The geochemistry of redox sensitive trace metals in sediments, *Geochim. Cosmochim. Acta*, *63*(11/12), 1735–1750, 1999.

Nägler, T. F., H.-J. Schäfer, and D. Gebauer, Evolution of the Western European continental crust: Implications from Nd and Pb isotopes in Iberian sediments, *Chem. Geol.*, *121*, 345–357, 1995.

Parrington, J. R., H. D. Knox, S. L. Brenemann, E. M. Baum, and F. Feiner (Eds.), *Nuclides and Isotopes, Chart of the Nuclides*, 64 pp., KAPL Inc., Lockheed Martin, Schenectady, N. Y., 1996.

Rehkämper, M., and A. N. Halliday, The precise measurement of Tl isotopic compositions by MC-ICPMS: Application to the analysis of geological materials and meteorites, *Geochim. Cosmochim. Acta*, *63*(6), 935–944, 1999.

Russell, W. A., D. A. Papanastassiou, and T. A. Tombrello, Ca isotope fractionation on the Earth and other solar system materials, *Geochim. Cosmochim. Acta*, *42*, 1075–1090, 1978.

Schoenberg, R., T. F. Nägler, and J. D. Kramers, Precise Os isotope ratio and Re-Os isotope dilution measurements down to the picogramm level using multicollector inductively coupled plasma mass spectrometry, *Int. J. Mass Spectrometry*, *197*, 85–94, 2000.

Stein, H. J., R. J. Markey, J. W. Morgan, A. Du, and Y. Sun, Highly precise and accurate Re-Os ages for molybdenite from the east Qinling molybdenum belt, Shaanxi Province, China, *Econ. Geol.*, *92*, 827–835, 1997.

Strelow, W. E., and C. J. C. Bothma, Anion exchange and a selectively scale for elements in sulfuric acid media with a strongly basic resin, *Anal. Chem.*, *39*(6), 595–599, 1967.

Sundius, Oil shale and shale oil industry, *Sveriges Geol., Ser. C*, *41*, 42, 1941.

von Blankenburg, F., and T. F. Nägler, Weathering versus circulation-controlled changes in radiogenic isotope tracer composition of Labrador Sea and North Atlantic Deep Water, *Paleoceanography*, in press, 2001.

White, W. M., F. Albarede, and P. Telouk, High-precision analysis of Pb isotope ratios by multi-collector ICP-MS, *Chem. Geol*, *167*(3–4), 257–270, 2000.

Wieser, M. E., and J. R. De Laeter, Thermal ionisation mass spectrometry of molybdenum isotopes, *Int. J. Mass Spectrometry*, *197*, 253–261, 2000.